Journal of Neuropathology and Experimental Neurology

Vol. 56, No. 2
February, 1997
pp. 171–179

Light and Electron Microscopic Analysis of the Central and Peripheral Nervous Systems of Acid Sphingomyelinase-deficient Mice Resulting from Gene Targeting

THOMAS ALFRED KUEMMEL, ROLAND SCHROEDER, AND WILHELM STOFFEL

Abstract. The acid sphingomyelinase (aSmase)-deficient mouse line recently generated by gene targeting (Otterbach and Stoffel, 1995) develops a lethal storage disease which is phenotypically comparable to the neurovisceral form of the human sphingomyelinosis, Niemann-Pick disease type A (NPA). This report describes the progressive accumulation of uncatabolized lipid substrates at the cellular and ultrastructural level in different regions of the nervous system of homozygous aSmase$^{-/-}$ mice, including cerebrum, cerebellum, spinal cord, optic nerve and peripheral nerves. We saw a cytoplasmic accumulation of pleomorphic lysosomal structures in cells of all regions under study, most extensively in macrophages, vascular endothelial cells, and also in neuronal perikarya. The complete and early degeneration of Purkinje cells was particularly striking. Moreover, we found a storage material in the cytoplasm of Schwann cells and to a minor extent in oligodendrocytes. In most advanced stages of the disorder, we detected an axonal dystrophy in both the central nervous system (CNS) and peripheral nervous system (PNS), without signs of dysmyelination or demyelination. The morphological changes of the central and peripheral nervous systems in the homozygous aSmase$^{-/-}$ mouse line closely resemble those in human NPA.

Key Words: Cytoplasmic inclusions; Histopathology; Knock-out mouse; Niemann-Pick disease; Ultrastructure.

INTRODUCTION

Niemann-Pick disease in its neurovisceral form, type A (NPA), or its visceral form, type B (NPB), is a lipidosis of autosomal recessive inheritance in man that results from a complete loss or a severe reduction of acid sphingomyelinase (aSmase) activity (0 to 10% of normal activity) (1–4). This enzyme is present in endosomes and lysosomes of all cells, but particularly in cells of the reticuloendothelial system of liver (Kupffer cells), spleen, bone marrow, and lung. In NPA, the sphingomyelin storage in these organs leads to hepatosplenomegaly and to severe involvement of both the central nervous system (CNS) and the peripheral nervous system (PNS), which results in a progressive loss of motor function and debility (5–7). Niemann-Pick disease patients have more severe symptoms and shorter life spans than NPB patients. The nosology of Niemann-Pick disease type C, which primarily leads to intracellular cholesterol storage (8), is totally different from NPA or NPB (9).

The enzyme aSmase has been isolated and characterized by cloning the cDNA (10) and determining the coding sequence of the human gene (11, 12). Different mutations, so far mostly point mutations, in the human aSmase gene have been found to cause either NPA or NPB (7, 13).

The recently isolated and characterized mouse and human aSmase genes are highly similar in size, organization, and nucleotide sequence of exons and introns (12). Starting with the isolated mouse aSmase gene, an acid-sphingomyelin-deficient mouse line was generated by use of the wild-type aSmase gene, in which exon III was disrupted by the insertion of the neomycin resistance gene for gene targeting by homologous recombination in embryonic stem cells (14). The genotype of this mouse model has been confirmed by Southern blot analysis and the lack of (aSmase$^{-/-}$) mRNA in liver, spleen, lung, and brain by Northern blot hybridization analysis. The complete absence of aSmase activity in all studied tissues was demonstrated by an enzyme assay with [N-$^{14}CH_3$]-sphingomyelin as the substrate. Preliminary analysis of the phenotype of the aSmase$^{-/-}$ mouse clearly indicated that this complete loss of aSmase leads to a neurovisceral storage disease corresponding to human NPA. The severe involvement of the nervous system and in particular the cerebellum of these animals, warranted a detailed analysis of CNS and PNS structures. Here we present a comprehensive study of the morphological changes in the central and peripheral nervous systems of the Niemann-Pick mouse (NPM).

MATERIALS AND METHODS

Animals

We employed homozygous offspring of the recently established aSmase$^{-/-}$ knock-out mouse line (14) in this study. We analyzed specimens of homozygous mice of different ages (18, 30, 43, 50, 65, 80, 100, 140, 210, and 225 days after birth) and from age-matched C57BL/6 control mice (one animal each) by light microscopy and partly by electron microscopy. Neurological findings were the same as reported for the animals selected by Otterbach and Stoffel (1995). In particular, we observed a generalized fine tremor and an increasing locomotor ataxy from weeks 8 to 10.

Processing for Light and Electron Microscopic Analysis

We euthanized wild-type and aSmase$^{-/-}$ mice using a CO_2 atmosphere. The right atrium of the heart was opened and the

From the Institute of Pathology (TK, RS) and the Institute of Biochemistry I (WS), Medical Faculty, University of Cologne, Germany.

Correspondence to: Wilhelm Stoffel, MD, PhD, Institute of Biochemistry, Medical Faculty, Joseph-Stelzmann-Str. 52, D-50931 Cologne, Germany.

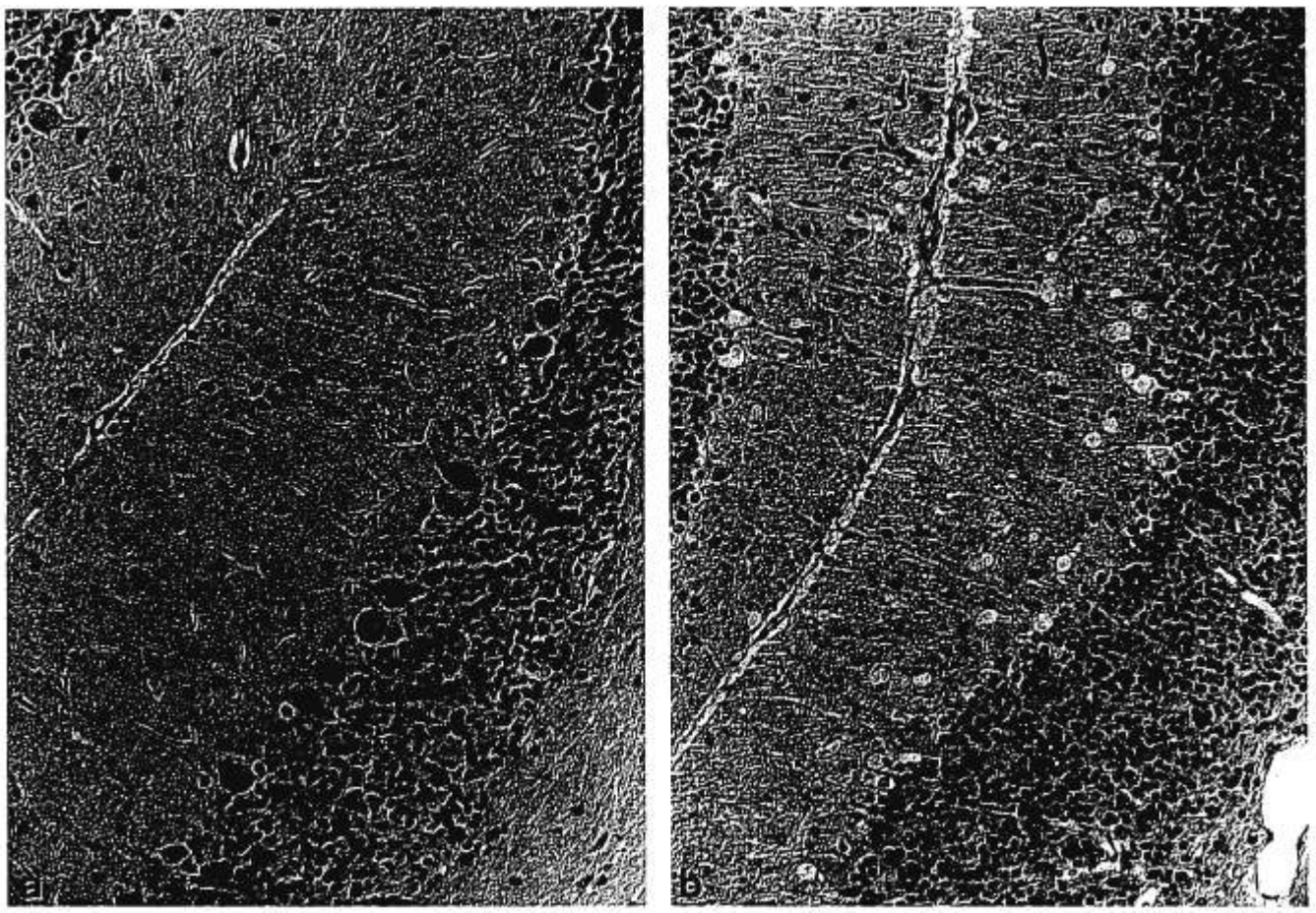

Fig. 1. Cerebellar cortex of the NPA mouse (light microscopy). a. 100-day-old wild-type animal with normal configuration of the cerebellar cortex. b. 100-day-old NPA mouse showing extensive reduction of Purkinje cells and numerous macrophages in the molecular layer. Luxol fast blue-cresyl violet, interference contrast, a, b, ×250.

mouse thoroughly perfused from the left ventricle with 20 ml of a mixture of glutardialdehyde (3%) and paraformaldehyde (2%) in 0.1 M phosphate buffered saline (PBS), pH 7.4. Then we prepared the brain, optic nerve (orbital part), spinal cord, and peripheral nerves (lumbosacral plexus). Additional fixation was done with 4% paraformaldehyde for paraffin histology and with 2.5% glutardialdehyde in 0.1 M sodium cacodylate buffer for specimens that were afterward embedded in araldite (24 hours [h] at 4 °C).

Fixed brains were not different in size in control and experimental animals. They were transversely sliced. We obtained specimens from cerebral hemispheres with corpus callosum, hippocampus, and basal ganglia, and from cerebellum and brainstem for histological examination; then we routinely embedded the samples in paraffin sectioned at 5 μm and stained with hematoxylin-eosin (HE), periodic acid-Schiff (PAS), Luxol fast blue-cresyl violet, and Palmgren's silver impregnation.

To determine the ultrastructure of different areas of the brain, optic nerve, and peripheral nerves, we fixed the following samples (0.5 to 1 mm^3 cubes) as described above, rinsed them in 0.1 M sodium cacodylate buffer, and postfixed them with 1% osmium tetroxide dissolved in the same buffer: cerebral cortex, cerebellar cortex, and spinal cord of the 100-day-old mouse; cerebellar cortex of the 18- and the 50-day-old mouse; spinal cord of the 18-day-old mouse; corpus callosum of the 210-day-old mouse; optic nerve of the 65- and 225-day-old mouse, and peripheral nerves from the lumbosacral plexus of the 210- and 225-day-old mouse. After postfixation, specimens were dehydrated in the ascending ethanol series and embedded in araldite. We mounted semithin sections (about 1.5

→

Fig. 2. Neuronal storage in cerebral and cerebellar cortex of the NPA mouse. a. Large neuron of the cerebral cortex of a 100-day-old animal containing numerous membrane-bound cytoplasmic bodies. b. Purkinje cell of an 18-day-old mouse with several lysosomal inclusions of stacked appearance (arrowheads) displaying close topographical vicinity to the Golgi apparatus (G). c. Purkinje cell of a 100-day-old animal with numerous lysosomes that disclose a pleomorphous appearance and mostly replace other cytoplasmic organelles. d. Magnification of lysosomes from c, containing electron-dense membraneous material in

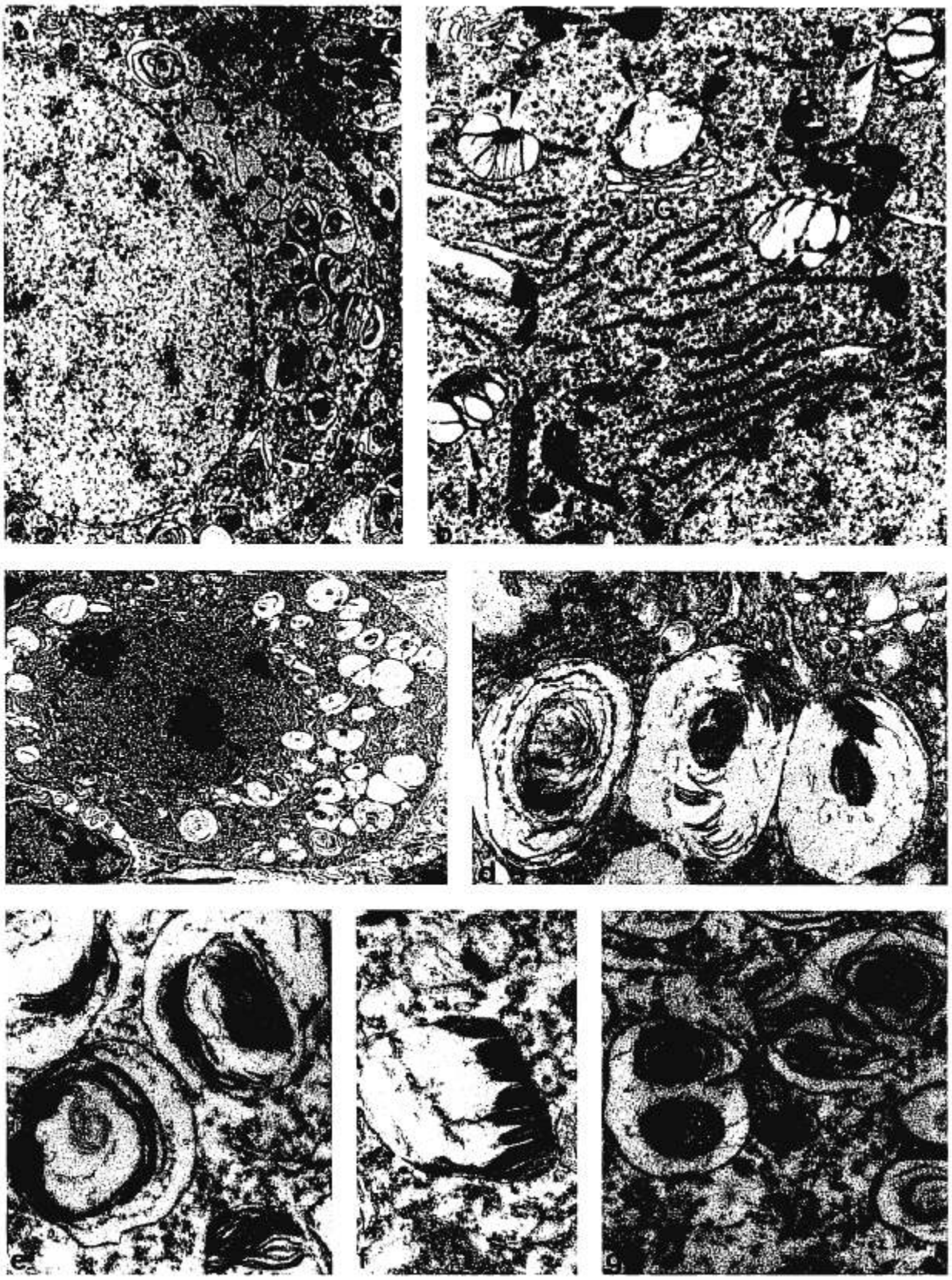

concentric lamellar arrangement. e–g. Pleomorphism of stored material in the 100-day-old NPA mouse with concentric (e) and stacked (f) arrangement as well as dense osmiophilic bodies, sometimes surrounded by loose membraneous lamellae (g). a, ×9,200; b, ×13,000; c, ×5,100; d, ×34,500; e-g, ×28,000.

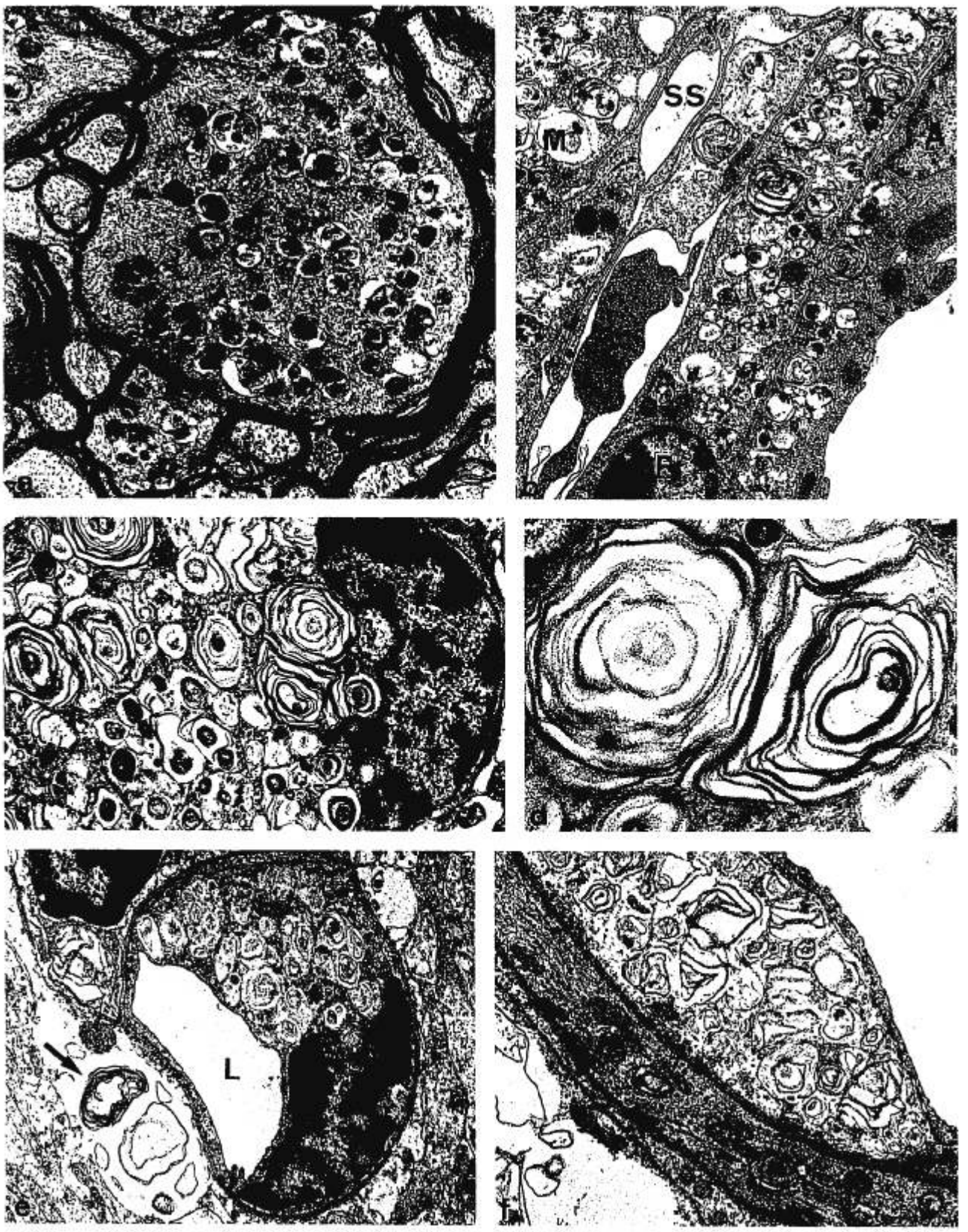

Fig. 3. White matter, meningeal cells, macrophages and endothelial cells of the CNS in NPA mice. a. Swollen myelinated axon of the optic nerve in a 225-day-old animal. There is a thinning of the myelin sheath and intraaxonal vacuolar and osmiophilic material. b. Meningeal sheath of the optic nerve of a mouse at day 65 with distinct cytoplasmic storage of membrane-bound

TABLE 1
Light Microscopical Findings of the Brain in Different Stages of the Disease

	Cerebral cortex		Cerebellar cortex			Corp call myelination
Age	v (N)	Ph	v (PC)	loss	Ph	
18 d	+	0	0	0	0	+
30 d	+	0	+	0	0	+
43 d	+	0	+	0	0	+
50 d	++	0	+	+	0	++
65 d	++	0	n a	n a	n a	++
80 d	+++	0	++	++	+	+++
100 d	+++	+	++	++	++	+++
140 d	+++	+	++	++	++	+++
210 d	+++	+	no PC	+++	++	+++
225 d	+++	+	no PC	+++	++	+++

Abbreviations: d = day, v = vacuolization, N = neurons, Ph = macrophages, corp call = corpus callosum, PC = Purkinje cells, n a = not available. Score of intensity: 0 = no, + = weak, ++ = moderate, +++ = strong.

μm) of all specimens on glass slides and stained them at 70 °C with an aqueous solution of 0.5% methylene blue in 0.5% borax/azur blue II. We mounted ultrathin sections (about 50 nm) on 200 mesh nickel grids and stained them by uranyl acetate (5 minutes [min]) and lead citrate (20 min).

RESULTS

A. Light Microscopy of CNS and PNS of the NPM Compared to Wild-type Controls

Examination of sequential sections of paraffin-embedded CNS tissue demonstrated a progressive vacuolar storage with increasing age of the animal (Table 1). This included all regions of the brain chosen randomly. A diffuse involvement of cerebral cortex with mild neuronal cytoplasmic vacuolization was already detectable at day 18 in the youngest animal studied. Storage progressed and neurons exhibited a foamy appearance around day 80. Vacuolization in neuronal cytoplasm was often associated with a slight swelling of the perikaryon and dendrites in advanced stages of the disease, most evident in large pyramidal cells. We did not observe a loss of neurons or gliosis in this region. The neurons of basal ganglia demonstrated storage starting on day 30.

Likewise, we detected an increasing vacuolization in the cytoplasm of the Purkinje and Golgi cells around day 30. A slight swelling of their perikarya and dendrites was a frequent finding in more advanced stages of the disorder. Loss of Purkinje cells beginning in the furrows of the hemispheres was evident from day 50, up to the total loss in both hemispheres and vermis at the age of 210 days (Fig. 1a, b). We detected a narrowing of the molecular layer starting on day 210, associated with a discrete increase of Bergmann glia. Silver impregnation did not reveal "torpedoes" of proximal Purkinje cell axons at any stage of the disorder. Deep cerebellar nuclei disclosed an increasing vacuolization of neurons from day 30, but there was no detectable neuronal loss.

Starting on day 210 we detected single axon swellings in the white matter of the cerebrum but not of the cerebellum. Macrophages with a foam-cell appearance occurred from day 100 in the cerebrum, and around day 80 in the cerebellar cortex, predominantly in the molecular layer (Fig. 1b). Some foam cells were visible at the outer rim of the deep cerebellar nuclei starting at 210 days of age. However, there was no obvious demyelination in the cerebellum or other regions of brain. Myelination of the CNS was regular and completed at day 80 (Table 1). Foamy macrophages and neurons were PAS negative.

In semithin sections Schwann cells in the PNS of 210- and 225-day-old animals contained dense cytoplasmic inclusions. We observed some swollen axons, while myelin sheaths seemed to be inconspicuous. These pathological changes in aSmase$^{-/-}$ mice were absent in C57BL/6 control mice.

B. Electron Microscopy in NPM and Wild-type Control Mice

The cytoplasmic inclusions in neurons of the cerebral cortex of the 100-day-old mouse were highly pleomorphic (Fig. 2a). Deposited uncatabolized lipid substrates formed either loosely coiled lamellar single membrane-bound material of varying compactness, stacked figures, or irregular membranous deposits of variable electron density. Moreover, electron-lucent vacuoles and osmiophilic bodies occurred (Fig. 2e–g). These storage products were observed in neuronal perikarya as well as in dendrites.

Purkinje cells showed lysosomal storage as early as day 18, with membrane-bound vacuoles closely attached to Golgi vesicles and endoplasmic reticulum (Fig. 2b). In advanced stages of the disorder (day 100), these organelles were almost completely replaced by lysosomes filled

←

material in arachnoidal cells (A), fibrocytes (F) and macrophages (M); subarachnoid space (SS). c. Foam cell of a 100-day-old mouse with marginalized nucleus and cytoplasm stuffed with numerous lysosomes often containing membraneous material in concentric arrangement or condensed osmiophilic inclusions. d. Details of membrane-bound bodies from c. e. Small cerebral capillary with eccentric cushion-like thickening of the endothelium stuffed with lysosomal storage material in an animal at day 100. Note the distinct narrowing of the vascular lumen (L) and the storage material in an astrocytic process (arrow). f. Arteriole of the same animal with endothelial storage material and smooth muscle cell containing single lysosomal inclusions (arrowhead). a, ×16,000; b, e, f, ×13,000; c, ×9,200; d, ×28,000.

with membraneous deposits (Fig. 2c), which in early stages (day 18, day 50) displayed a mostly stacked morphology (Fig. 2b). Around day 100, the membrane-bound inclusions were condensed to form electron-dense material, often with lamellar arrangement (Fig. 2g). Golgi neurons of 100-day-old animals displayed numerous vacuolar inclusions, whereas granule cells mostly revealed a few membrane-bound bodies with loose amorphous or lamellar membranous material. In neuronal perikarya of the spinal cord, lysosomal inclusions were already detectable at day 18.

Single myelinated nerve fibers in the white matter of cerebrum, but not of the cerebellum of the 210-day-old animal, and, more frequently, in the optic nerve of the 225-day-old NPA mouse, disclosed axonal dystrophy with marked swelling and thinning of the myelin sheath (Fig. 3a). Axons were stuffed with osmiophilic and vesicular structures that were morphologically different from storage lysosomes of the perikarya. We did not find similar changes in the white matter of the cerebrum or in the cerebellum of 100-day-old animals or in the optic nerve of the 65-day-old mouse.

Meningeal cells, i.e. arachnoidal cells, fibrocytes, endothelial cells, and vascular pericytes, as well as macrophages, displayed all distinct storage phenomena at early stages of the disorder (Fig. 3b). The cytoplasm of macrophages within the parenchyma of the 100-day-old mouse was stuffed with lysosomes containing pleomorphic storage material, mostly coiled membraneous structures (Fig. 3c, d). Astrocytes and oligodendrocytes in all brain regions examined had similar inclusion bodies (Fig. 3e), but in lower numbers. Endothelial cells of small blood vessels throughout the brain revealed cytoplasmic storage of heterogenous membrane-bound subcellular vesicles and osmiophilic inclusions (Fig. 3f), often with marked narrowing of the vessel lumen (Fig. 3e). Single storage bodies were found in vascular smooth muscle cells (Fig. 3f).

Schwann cells of peripheral nerves of the 210- and 225-day-old animals stored mostly vesicular and also stacked membraneous osmiophilic material in the cytoplasm (Fig. 4a, b). Occasionally, unmyelinated and myelinated axons showed dystrophic swellings containing vesicular and dense granular structures (Fig. 4c, d) equivalent to those observed in central axons. Cells of the endoneural connective tissue of peripheral nerves showed changes similar to those in meningeal cells. Age-matched C57BL/6 control mice did not show any of the pathological changes of the NPM.

DISCUSSION

Several mouse strains were selected as models for human Niemann-Pick disease, including the NCTR-Balb/c mouse (15), mutant substrains of C57 BL/KsJ mice (16), and CBA mice–fm/fm (17). These models were studied carefully, and methods including mutation analysis and chromosomal mapping clearly indicate a mimicry of Niemann-Pick disease type C (NPC) (18). A similar model resembling NPA was not available and only a few cases of animals with severe aSmase deficiency corresponding to human NPA, i.e. in dogs (19) and cats (20, 21), have been reported. Recently, two mouse models with defined enzyme defects that mimic human Niemann-Pick disease type A have been established employing the technique of gene targeting by homologous recombination and are referred to below as M-1 (14) and M-2 (22).

These $Smase^{-/-}$ knock-out mice develop a similar pathology within 8 to 10 weeks. Symptoms are tremor and ataxia. They have a similar life expectancy of around 6 to 8 months. Ataxia and dysmetria indicating severe cerebellar dysfunction are also major symptoms in canine (19) and feline sphingomyelinosis (20, 23), but are of minor importance in man (5–7). On the other hand, certain differences between these models are evident. Thus, hepatosplenomegaly, an impressive symptom in human Niemann-Pick disease (5, 7), was also obvious in the model studied here (M-1) and in canine (19) and feline sphingomyelinosis (20), but was lacking in M-2. Studies of enzyme activity displayed a total loss of aSmase activity in both models. Corresponding to studies in humans (24) as well as in the feline NPA model of Wenger (1980), residual neutral sphingomyelinase activity in brains of M-1 animals is almost identical with age-matched wild-type mice, whereas it is decreased by 50% in M-2. The reduced activity observed in the latter model was alleged to be secondary to the abnormal cell pathology and lipid accumulation in the brains of affected animals rather than to a primary defect in the enzyme (22). In M-2, brains of animals at the time of death were less than half the weight and volume of controls and in particular a general atrophy of cerebellum and midbrain was evident in addition to a remarkable loss of Purkinje cells. In contrast, animals of M-1 did not show any major differences with regard to brain volume when compared to age-matched controls and present a selective loss of Purkinje cells with a discrete narrowing of the molecular cell layer in final stages of the disorder (day 210, day 225). At autopsy, brains of human NPA patients indicate a distinct atrophy (25) with markedly reduced weight.

While neuronal storage is often found to be accompanied by a progressive cell degeneration (5), a selective loss of Purkinje cells was not reported in man. On the other hand, Purkinje cell degeneration or apoptosis was also observed in canine sphingomyelinosis (19) and in a number of different mutant animals with neurological deficits (26–30).

The underlying mechanisms of cell degeneration in storage disorders are not clearly understood. The voluminous lysosomal deposits in the ER and Golgi complex may impair dendritic growth and formation of synapses

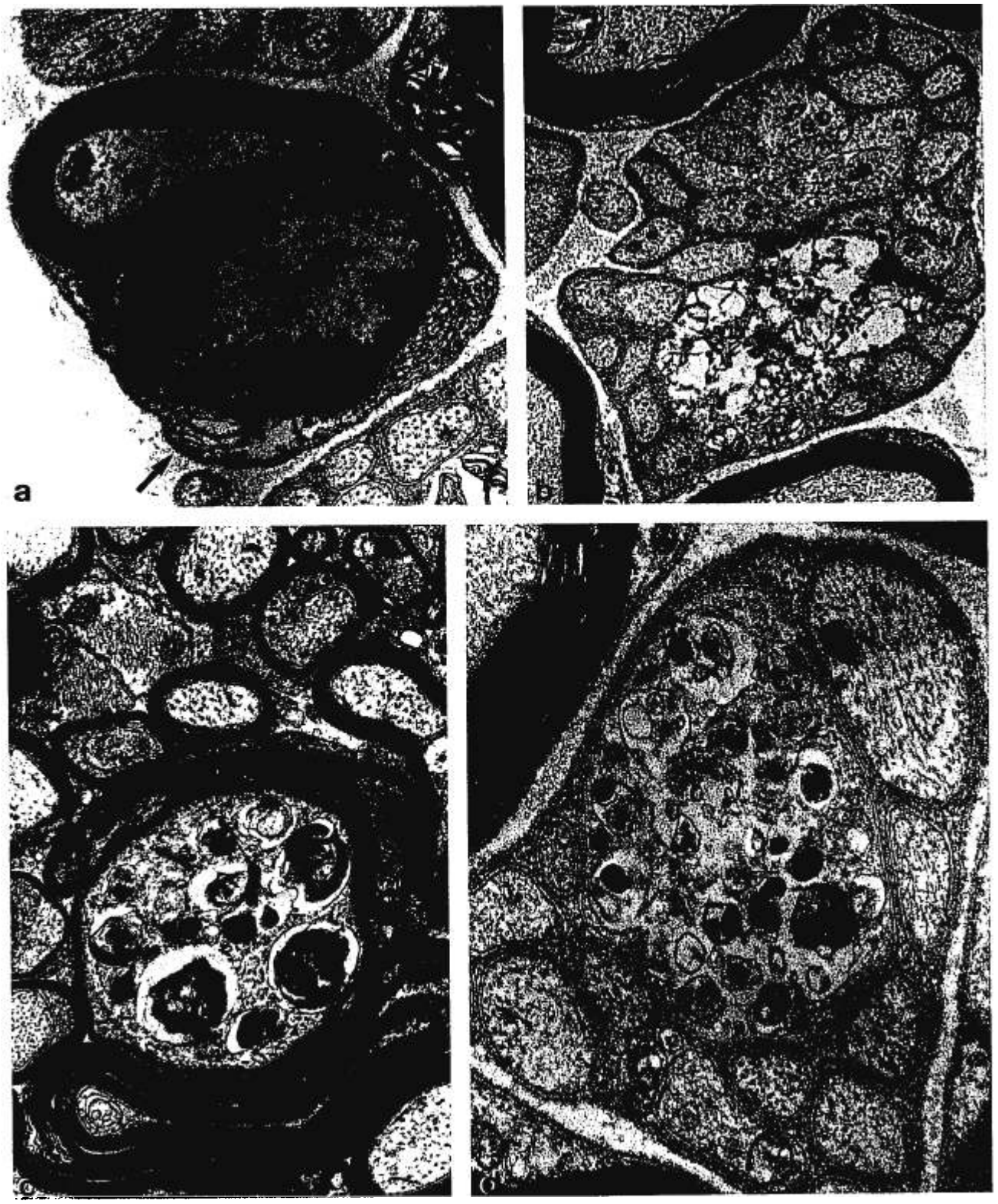

Fig. 4. Peripheral nerve of the Niemann-Pick mouse. a. Schwann cell of myelinated axon of the 210-day-old animal with single lysosomal inclusions of stacked arrangement (arrow). b. Unmyelinated nerve fiber of the same animal with loose membraneous and vesicular material in Schwann cell cytoplasm. c. Myelinated swollen axon of an animal at day 225 containing electron-dense and loose vesicular bodies and displaying thinning of the myelin sheath. d. Unmyelinated axon of a 210-day-old mouse revealing axonal swelling filled with material similar to the myelinated axon shown in c. a, d, ×22,000; b, ×13,000; c, ×27,000.

and finally result in cell death (31). Furthermore, cytotoxic events induced by a perturbed cellular metabolism may result in impaired membrane transport (30).

It is tempting to speculate that the preferred degeneration of cerebellar Purkinje cells compared to other neurons in the brain is due to their neuronal activity, which exceeds that of most other cell types. This is reflected by their high number of dendritic processes and synaptic connections (32). In this context it should be mentioned that Purkinje cells of the sphingomyelinosis mouse strain fail to express the membrane-bound glycoprotein P400 before degeneration (33). This glycoprotein is involved in the synaptogenesis and morphogenesis of Purkinje cells (34). Its lack of expression indicates abnormalities of the membrane with distortion of dendritic processes or synaptic junctions. The loss of Purkinje cells according to a strict topographical sequence that is the same for both NPA and NPC mice (30) is another unexplained phenomenon.

Sensitive ultastructural analyses allow detection of lysosomal storage at an early age in aSmase-deficient mice. This early morphological manifestation is a well-known phenomenon in human neurolipidoses. Membraneous inclusions were found in several fetal tissues after abortion (35–37).

However, the significance of the ultrastructural appearance of stored material in lysosomes for subclassification of different metabolic disorders is questionable (38). In our study of the NPA mouse strain, we observed a pleomorphism of storage figures in advanced stages of the disease in all regions of mouse brain and a linkage between the number of neuronal lysosomes, and increased pleomorphism of deposited membrane-bound material with time (Fig. 2e–g).

In agreement with a few ultrastructural studies of the peripheral nervous system in human NPA (39–41), we observed membrane-bound storage material of vesicular and granular appearance in the cytoplasm of Schwann cells. Axonal degeneration has been reported in NPA consisting of a reduction or loss of normal neurofilaments and their replacement by loose floccular material (40), but this is more frequent and severe in NPC (42, 43). In our model a distinct axonopathy with dystrophic swellings in both unmyelinated and myelinated peripheral axons was more pronounced than in central axons and only detected in late stages of the disorder. On the other hand, the severe myelinopathy described in human NPA (41) was not present in either the PNS or the CNS of the mouse model.

In conclusion, the morphological investigations of M-1 described here unambiguously demonstrate that the a-Smase null allelic mouse generated by gene targeting using homologous recombination represents an animal model of the sphingomyelin storage disease that mimicks the human NPA. However, careful comparison involving biochemical and morphological criteria displayed minor differences between both mice models of NPA (M-1 and M-2), several case reports of this disorder in other species (cat, dog), as well as the neurovisceral form of the Niemann-Pick disease in man. Our asmase$^{-/-}$ mouse line (Otterbach and Stoffel, 1995) is a genetically, biochemically, and now also a neuropathologically well-defined animal model that provides the opportunity to study pathophysiological mechanisms underlying clinical symptoms, the pathogenesis of nerve cell degeneration, and the importance of acid sphingomyelinase in the TNFa-TNFa receptor NF-kB signal transduction (44), and to develop and test new basic therapeutic strategies, among them gene therapy.

ACKNOWLEDGMENTS

Supported by the Deutsche Forschungsgemeinschaft project Sto 32/36-1 and by the BMBF, "Gesundheitsforschung 2000," Interdisciplinary Center of Clinical Research, project 24. The authors thank Mrs E. Varus and Mrs M. Düker for excellent technical assistance.

REFERENCES

1. Niemann A. Ein unbekanntes Krankheitsbild. Jahrb Kinderheilkd. 1914;79:1–10
2. Klenk E. Über die Natur der Phosphatide und anderer Lipide des Gehirns und der Leber bei der Niemann-Pick-Krankheit. Hoppe-Seyler's Z Physiol Chem 1935;235:24–36
3. Pick L. Über die lipoidzellige Splenohepatomegalie Typus Niemann-Pick als Stoffwechselerkrankung. Med Klin 1927;23: 1483–88
4. Brady RO, Kanfer JN, Mock MB, Fredrickson DS. The metabolism of sphingomyelin, II. Evidence of an enzymatic deficiency in Niemann-Pick disease. Proc Natl Acad Sci USA 1966;55:366–69
5. Elleder M. Niemann-Pick disease. Pathol Res Pract 1989;185:293–28
6. Lake BD. Lysosomal and peroxisomal disorders. In: Adams JH, Duchen LW, eds. Greenfield's neuropathology. London: Hodder and Stoughton, 1994:709–810
7. Schuchman EH, Desnick RJ. Niemann-Pick disease types A and B: Acid sphingomyelinase deficiencies. In: Scriver CR, Beaudet AL, Sly WS, Valle D, eds. The metabolic and molecular basis of inherited disease. New York: McGraw-Hill, Inc, 1995:2601–24
8. Vanier MT, Rodriguez-Lafrasse C, Rousson R, et al. Type C Niemann-Pick disease: Biochemical aspects and phenotypic heterogeneity. Dev Neurosci 1991;13:307–14
9. Crocker AC. The cerebral defect in Tay-Sachs disease and Niemann-Pick disease. J Neurochem 1961;7:69–80
10. Quintern LE, Schuchman EH, Levran O, et al. Isolation of cDNA clones encoding human acid sphingomyelinase: Occurrence of alternatively processed transcripts. EMBO J 1989;8:2469–73
11. Schuchman EH, Suchi M, Takahashi T, Sandhoff K, Desnick RJ. Human acid sphingomyelinase. Isolation, nucleotide sequence, and expression of the full-length and alternatively spliced cDNAs. J Biol Chem 1991;266:8531–39
12. Newrzella D, Stoffel W. Molecular cloning of the acid sphingomyelinase of the mouse and the organization and complete nucleotide sequence of the gene. Hoppe-Seyler's Z Biol Chem 1992: 373;1233–38
13. Weisz B, Spirer Z, Reif S. Niemann-Pick disease: Newer classification based on genetic mutations of the disease. Adv Pediat 1994;41:415–26

14. Otterbach B, Stoffel W. Acid sphingomyelinase-deficient mice mimic the neurovisceral form of human lysosomal storage disease (Niemann-Pick disease). Cell 1995;81:1053–61
15. Morris MD, Bhuvaneswaran C, Shio H, Fowler S. Lysosome lipid storage disorder in NCTR-BALB/c mice. Am J Pathol 1982;108: 140–49
16. Miyawaki S, Mitsuoka S, Sakiyama T, Kitagawa T. Sphingomyelinosis, a new mutation in the mouse. J Hered 1982;73:257–63
17. Lyon MF, Hulse EV, Rowe CE. Foam-cell reticulosis of mice: An inherited condition resembling Gaucher's and Niemann-Pick diseases. J Med Genet 1965;2:99–106
18. Horinouchi K, Sakiyama T, Pereira L, Lalley PA, Schuchman EH. Mouse models of Niemann-Pick disease: Mutation analysis and chromosomal mapping rule out the type A and B forms. Genomics 1993;18:450–51
19. Bundza A, Lowden JA, Charlton KM. Niemann-Pick disease in a poodle dog. Vet Pathol 1979;16:530–38
20. Wenger DA, Sattler M, Kudoh T, Snyder SP, Kingston RS. Niemann-Pick disease: A genetic model in Siamese cats. Science 1980;208:1471–73
21. Walkley SU, Baker HJ. Sphingomyelin lipidosis in a cat: Golgi studies. Acta Neuropathol 1984;65:138–44
22. Horinouchi K, Erlich S, Perl DP, et al. Acid sphingomyelinase deficient mice: A model of types A and B Niemann-Pick disease. Nat Genet 1995;10:288–93
23. Baker HJ, Wood PA, Wenger DA, et al. Sphingomyelin lipidosis in a cat. Vet Pathol 1987;24:386–91
24. Wenger DA, Wharton C, Sattler M, Clark C. Niemann-Pick disease: Prenatal diagnoses and studies of sphingomyelinase activities. Am J Med Genet 1978;2:345–56
25. Crocker AC, Farber S. Niemann-Pick disease: A review of eighteen patients. Medicine 1958;37:1–95
26. Meier H, MacPike AD. Three syndromes produced by two mutant genes in the mouse. J Hered 1971;61:297–302
27. Landis SC. Ultrastructural changes in the mitochondria of cerebellar Purkinje cells of nervous mutant mice. J Cell Biol 1973;57:782–97
28. Mullen RJ, Eicher EM, Sidman RL. Purkinje cell degeneration, a new neurological mutation in the mouse. Proc Natl Acad Sci USA 1976;73:208–12
29. Tanaka J, Nakamura H, Miyawaki S. Cerebellar involvement in murine sphingomyelinosis: A new model of Niemann-Pick disease. J Neuropathol Exp Neurol 1988;47:291–300
30. Higashi Y, Murayama S, Pentchev PG, Suzuki K. Cerebellar degeneration in the Niemann-Pick type C mouse. Acta Neuropathol 1993;85:175–84
31. Schulte FJ. Clinical course of GM2 gangliosidoses–a correlative attempt. Neuropediatrics Suppl 1984;15:66–70
32. Konnerth A, Llano I, Armstrong CM. Synaptic currents in cerebellar Purkinje cells. Proc Natl Acad Sci USA 1990;87:2662–65
33. Tanaka J, Miyawaki S, Maeda N, Mikoshiba K. Immunohistochemical expression of P400 protein in Purkinje cells of sphingomyelinosis mouse. Brain Dev 1991;13:110–14
34. Maeda N, Niinobe M, Inoue Y, Mikoshiba K. Developmental expression and intracellular location of P400 protein characteristic of Purkinje cells in the mouse cerebellum. Dev Biol 1989;133:67–76
35. Schneider EL, Ellis WG, Brady RO, McCulloch JR, Epstein CJ. Prenatal Niemann-Pick disease: Biochemical and histologic examination of a 19-gestational week fetus. Pediatr Res 1972;6:720–29
36. Suchlandt G, Schlote W, Harzer K. Ultrastrukturelle Befunde bei 9 Feten nach pränataler Diagnose von Neurolipidosen. Arch Psychiatr Nervenkr 1982;232:407–26
37. Dumontel C, Girod C, Dijoud F, Dumez Y, Vanier MT. Fetal Niemann-Pick disease type C: Ultrastructural and lipid findings in liver and spleen. Virch Arch A Pathol Anat Histopathol 1993;422: 253–59
38. Suzuki K. Metabolic diseases. In: Johannessen JV, ed. Electron microscopy in human medicine. New York: McGraw-Hill, 1979;6:3–53
39. Da Silva V, Vassella F, Bischoff A, Spycher M, Wiesmann UN, Herschkowitz N. Niemann-Pick's disease. Clinical, biochemical and ultrastructural findings in a case of the infantile form. J Neurol 1975;211:61–68
40. Gumbinas M, Larsen M, Liu HM. Peripheral neuropathy in classic Niemann-Pick disease: Ultrastructure of nerves and skeletal muscles. Neurology 1975;25:107–13
41. Landrieu P, Said G. Peripheral neuropathy in type A Niemann-Pick disease. Acta Neuropathol 1984;63:66–71
42. Jellinger K, Jirasek A. Neuroaxonal dystrophy in man: Character and natural history. Acta Neuropathol Suppl 1971;5:3–16
43. Hahn AF, Gilbert JJ, Kwarciak C, et al. Nerve biopsy findings in Niemann-Pick type II (NPC). Acta Neuropathol 1994;87:149–54
44. Kolesnick R, Golde DW. The sphingomyelin pathway in tumor necrosis factor and interleukin-1 signaling. Cell 1994;77:325–28

Received March 26, 1996
Revision received July 30, 1996
Accepted November 1, 1996